

THE PENNSYLVANIA STATE UNIVERSITY
SCHREYER HONORS COLLEGE

DEPARTMENT OF BIOCHEMISTRY AND MOLECULAR BIOLOGY

Exploring the Specialization of Expansion Segments in
Temporally Expressed *Plasmodium* Ribosomes

LEENA WARDEH
SPRING 2024

A thesis
submitted in partial fulfillment
of the requirements
for a baccalaureate degree
in Biology - Vertebrate Physiology
with honors in Biology

Reviewed and approved* by the following:

Dr. Scott E. Lindner
Associate Professor of Biochemistry and Molecular Biology
Thesis Supervisor

Dr. Timothy Jegla
Associate Professor of Biology, Associated Department Head of Graduate Education
Honors Adviser

* Electronic approvals are on file.

ABSTRACT

Malaria, a deadly disease caused by the *Plasmodium* parasite, remains a significant threat to public health worldwide. Developing effective drugs to combat malaria is challenging due to the parasite's ability to rapidly develop resistance to antimalarials, as seen with existing medications such as chloroquine, quinine, sulfadoxine, and halofantrine. However, a potential target for novel antimalarials lies in the unique, heterogenous ribosomes found in *Plasmodium*, and their temporally expressed Asexual (A) and Sporozoite (S) types. These ribosomes contain sequence variations between their rRNAs, particularly in expansion segments (ESs), which are protrusions of ribosomal RNA (rRNA) sequences outside the conserved core rRNA. While the functional roles of eukaryotic ESs are not fully understood, they play crucial roles in ribosome biogenesis and recruit specific effector proteins acting on nascent polypeptides. This evidence of rRNA ES interactions with ribosome-associated factors in eukaryotes leads me to hypothesize that certain rRNAs varying between A- and S-type ribosomes may interact with a protein complex crucial for *Plasmodium* ribosome specialization. The aim of this project was to develop a reproducible protocol to generate ES probes identical in size and sequence to *Plasmodium's* ES9S and ES27L sequences that protrude from A-type and S-type ribosomes. I established the experimental workflow by exclusively focusing on creating control ES GFP RNA probes designed to mirror the approximate sequence length and predicted structure of the three sequences for both the *P. yoelii* ES9S sequence and ES27L sequence, located on Chromosomes 5, 6, and 12. These ESs were chosen for investigation because of their demonstrated specialized functions in other eukaryotic organisms. Throughout this project, I established a reliable and consistent protocol for generating these RNAs that can be applied to the remaining ES RNA probes chosen for this study. This will enable efforts to determine whether the other six ES9S

and ES27L A-type and S-type ES possess the capacity to selectively bind effector proteins. These results would demonstrate their specialized translational function in *Plasmodium*, which could advance understanding of stage-specific *Plasmodium* ribosomes and their role in translational regulation throughout the malaria life cycle. Through the generation of ES RNA probes known to have specialized functions in other eukaryotic organisms, we aim to uncover whether similar specialized functions exist in *Plasmodium*, potentially offering valuable targets for vaccines or medications focused on disrupting the translational dynamics of malaria.

TABLE OF CONTENTS

LIST OF FIGURES	v
LIST OF TABLES.....	vi
ACKNOWLEDGEMENTS.....	vii
Chapter 1 Introduction	1
1.1 Malaria's Real-World Relevance	1
1.2 The Complex Life Cycle of <i>Plasmodium</i>	2
1.3 Ribosome Heterogeneity and Specialization	4
1.4 Evidence for <i>Plasmodium</i> Ribosome Specialization	5
1.5 Application of Temporally Expressed Expansion Segments.....	7
1.6 Goals and Hypothesis of <i>Plasmodium yoelii</i> ES9S and ES27L Experiments	9
1.7 Experimental Overview	10
Chapter 2 Materials and Methods.....	13
2.1 Synthesizing <i>Plasmodium yoelii</i> Plasmids	13
2.2 Transforming and Purifying Plasmids	14
2.3 Picking Colonies	14
2.4 Plasmid DNA Midiprep	15
2.5 Midiprep Finalizer	16
2.6 Linearizing ES Plasmids.....	16
2.7 Transcribing Linearized DNA via T7 RNA Polymerase.....	17
2.8 Separating ES RNA via 8% SDS Polyacrylamide Gel.....	18
2.9 Extracting and Purifying GFP RNA via Electroelution.....	19
2.10 Qubit RNA HS Assay	20
2.11 Biotin Labeling and Purifying GFP RNA.....	20
2.12 Dot Blot Analysis of Biotinylated RNA	21
2.13 Synthesizing Human Dicer Proteins	22
2.14 Protein Binding Confirmation using EMSA.....	23
Chapter 3 Results	24
3.1 Verification of Transforming and Transcribing ES DNA	24
3.2 Confirmation of the Production and Purification of ES RNA	26
3.3 Confirmation of Biotinylating ES RNA	29
3.4 Confirmation of ES RNA Binding to Proteins	29
Chapter 4 Discussion	32
4.1 The established methodology for generating ES probes is reproducible and effective	32
4.2 Successfully establishing a preliminary protocol with GFP ES RNA.....	34
4.3 hDicer as a positive control spike-in protein for future proteomics	34

4.4 Future Directions for Generating ES Probes	36
4.4.1 Incorporating the streptavidin binding protocol into biotinylated ES dsRNA probes	36
4.4.2 Utilizing Plasmodium yoelii Parasite Lysate	37
4.4.3 Potential Pitfalls and Alternate Approaches	39
4.5 Summary	40
BIBLIOGRAPHY	42

LIST OF FIGURES

Figure 1. Malaria Transmission by Country (CDC, 2020).....	1
Figure 2. <i>Plasmodium</i> Life Cycle (CDC, 2002).....	3
Figure 3. A-Type and S-Type Ribosome Expression throughout <i>P. yoelii</i> Life Cycle Stages (McGee, 2019).....	7
Figure 4. ChimeraX model of <i>Plasmodium falciparum</i> A-type Ribosome and Predicted Secondary Structures of A-type and S-type ES9S and ES27L (McGee, 2023)	8
Figure 5. An illustration of ES9S A-Type versus S-Type bound to biotin. The non-covalent interaction between streptavidin is indicated in dashed lines. Proteins X and Y mimic currently unidentified proteins of interest (Wardeh, 2023).	10
Figure 6. 1% Agarose Gel Confirming Linearization of Selected ES9S and ES27L Plasmid DNA25	
Figure 7. Confirmation of Transcribing ES RNA from ES DNA using Chr6S-ES27L and Control GFP DNA Templates using an 8% SDS Polyacrylamide Gel.....	27
Figure 8. Confirmation of Biotinylated Control GFP ES dsRNA using Dot Blot Analysis ..	29
Figure 9. Confirmation of Human Dicer Protein binding to Biotinylated Control GFP ES dsRNA using EMSA.....	30

LIST OF TABLES

Table 1. The selected <i>Plasmodium yoelii</i> ES DNA Sequences on Chromosomes 5, 6, 12, and Control GFP.	24
Table 2. Concentrations of <i>Plasmodium yoelii</i> Expansion Segment (ES) linearized DNA.	26

ACKNOWLEDGEMENTS

I would like to thank my thesis supervisor, Dr. Scott E. Lindner, for the opportunity to work in the Lindner Laboratory for the last two years of my undergraduate education. I want to also thank my mentors James P. McGee and Allen Minns, who guided me throughout my thesis project and taught me how to apply myself like a true biologist. Lastly, I would like to thank all the other members of the Lindner Lab for everything they have done to further our understanding of malaria. I would like to acknowledge my sources of funding, including the Schreyer Honors College Thesis Grant, the Penn State Office of Science Engagement Research Grant, and the Erickson Discovery Grant, which allowed me to stay in the summer to further my research. Finally, I would like to thank my family and friends in the Schreyer Honors College and Penn State University Park campus who have supported me throughout this project.

Chapter 1

Introduction

1.1 Malaria's Real-World Relevance

Malaria, an infectious disease caused by the *Plasmodium* parasite, is one of the oldest and deadliest diseases that remains a public health threat worldwide. According to the 2023 World Health Organization Malaria Report, over 249 million malaria cases were recorded in 2022, leading to death for 608,000 individuals [1]. Malaria is a leading cause of death in several developing countries, impacting health standards negatively for the world at large. Malaria poses a large threat to several areas of sub-Saharan Africa, due to the conducive weather and environment for mosquito breeding, the invertebrate vector required for the lifespan and transmission of *Plasmodium*, compounded by the limited protection against mosquito bites in the region (Figure 1.1). Individuals most affected by the disease include pregnant women, children, and elderly populations.

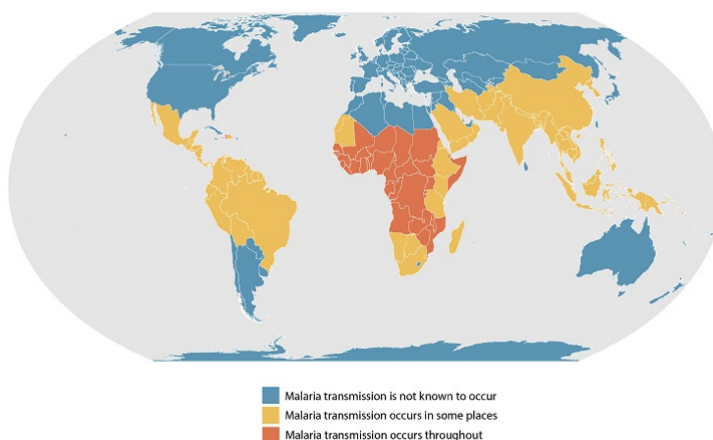


Figure 1. Malaria Transmission by Country (CDC, 2020)

It is incredibly challenging to develop an effective drug to prevent malaria outbreaks amongst these populations due to the ability of *Plasmodium* to rapidly develop resistance to antimalarial drugs. Species such as *P. falciparum* and *P. vivax* have developed resistance to antimalarial drugs such as chloroquine, quinine, sulfadoxine, and halofantrine, making it imperative to find novel drugs that can offset parasitic resistance [2]. Currently, effective treatments for malaria have been the use of combination therapies that target multiple essential processes, which still require a firm knowledge of pathogen biology [3]. The intricate life cycle of *Plasmodium* also significantly contributes to the challenges in developing drugs, as *Plasmodium* differentiates through several stages in both human hosts and mosquito vectors. Developing drugs that can address different and specific stages while minimizing human side effects and ensuring efficacy poses a considerable challenge in the pursuit of effective malaria prevention. In order to develop drugs that can both address different and specific stages of the parasite while minimizing human side effects while ensuring efficacy, unique and targetable characteristics of the parasite's cell biology need to be investigated.

1.2 The Complex Life Cycle of *Plasmodium*

As seen in Figure 2, the full *Plasmodium* life cycle occurs in a mammalian host as well as a female *Anopheles* mosquito vector. The infected mosquito will bite a mammalian host to collect a blood meal while simultaneously injecting sporozoites into the mammalian skin. The sporozoites travel to the vasculature system to passively travel to hepatocytes of the liver to initiate the exoerythrocytic stage of the cycle. Inside hepatocytes, sporozoites undergo asexual reproduction forming a liver-stage schizont, which ruptures and releases thousands of merozoites

into the bloodstream to infect red blood cells (RBCs). The parasites develop from an immature asexual ring to a mature trophozoite, which becomes a schizont that releases 6-24 merozoites to invade more RBCs. This infectious cycle of invasion, replication, and release leads to the clinical presentation of malaria, the destruction of red blood cells, and mammals begin to display physical symptoms of illness (anemia and immune system responses).

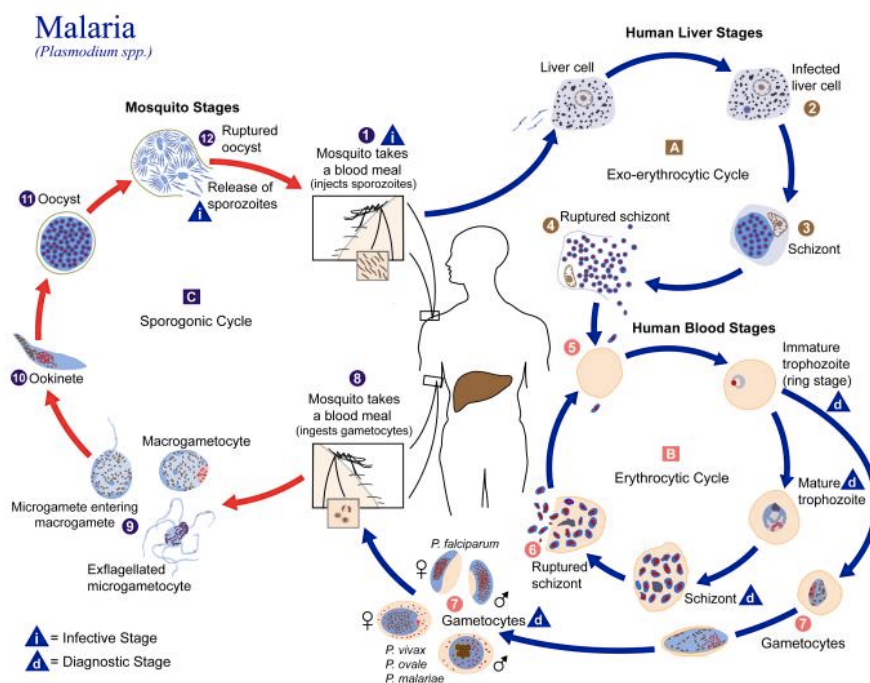


Figure 2. *Plasmodium* Life Cycle (CDC, 2002)

A subset of asexual blood-stage parasites can also differentiate to form sexual-stage parasites (known as gametocytes), which can be transferred from mammalian hosts to productively infect mosquitos through another blood meal. *Plasmodium* gametocytes undergo gametogenesis to form male and female gametes, which fuse to form a zygote in the mosquito midgut. Zygotes must become motile to escape the digestive processes of the midgut, and thus form an ookinete that burrows into the midgut wall and forms an oocyst under the basal lamina. The oocyst forms sporozoites within it, which then travel to the salivary glands after bursting

from the oocyst. Once the sporozoites reach the salivary glands and the mosquito begins to probe for another mammalian blood meal, the cycle begins again.

1.3 Ribosome Heterogeneity and Specialization

Ribosomes are the organelles responsible for protein synthesis, known as translation, and play an essential role in expressing the genetic makeup of all living organisms. Over the last few decades, advancements in molecular studies have refuted the notion that ribosomes are all effectively the same in form and function. Instead, research revealed that ribosomes are heterogeneous, meaning they are of various compositions of protein and RNA molecules that give them their mixed nature [4]. Ribosome heterogeneity allows these organelles to possess diverse ribosomal protein (RP) and ribosome-associated protein (RAP) compositions, suggesting their potential to express specific RP paralogs in different tissues and organs [5].

Although core rRNA has remained highly conserved across species, different eukaryotic species developed their own unique rRNA sequences known as expansion segments (ES). Expansion segments are protrusions of rRNA from the core rRNA framework possessing species-specific variations in length and structure [6]. While knowledge of the functional roles of eukaryotic ESs is limited, it is known that they play an essential role in eukaryotic ribosome biogenesis [7], recruitment of Ribosome Proteins (RPs), and specific effector proteins that can act on nascent polypeptides [8]. Few studies have already located ribosome specialization in ESs that contribute to ribosome heterogeneity [9]. Two of these that have been well characterized are ES27L (Expansion Segment 27 Large subunit) and ES9S (Expansion Segment 9 Small subunit). ES27L was seen in "humanized" yeast to act as an RNA scaffold that facilitated the binding of ribosome-associated protein MetAP (methionine amino peptidase), a conserved enzyme that is

essential for its role in translation fidelity [8]. Additionally, ES9S was observed in yeast to provide a means for Hoxa9 mRNA to bind to yeast ribosomes, an essential RNA regulator of eukaryotic body plan formation [10].

1.4 Evidence for *Plasmodium* Ribosome Specialization

The ribosomes of *Plasmodium* species have long been used as an example of ribosome heterogeneity and could be used as a target for developing antimalarial drugs. Exploiting specialized molecular mechanisms specific to *Plasmodium* that do not occur in the mammalian host is essential in developing an antimalarial drug that is both effective and reproducible. A potential target is found in the essential and atypical nature of the ribosomes found in *Plasmodium*—two ribosome types with temporally different expression patterns [5]. Contrary to almost all other eukaryotes, *Plasmodium* species only code for a handful of rDNA loci that code for the rRNA needed to make two temporally regulated ribosome forms: the Asexual type (A-type) and the Sporozoite type (S-type) [11]. For example, in rodent-infectious species *P. yoelii* and *P. berghei*, there are only four rDNA loci located on different chromosomes [5]. This is an atypical contrast to other eukaryotic organisms, which code for hundreds to thousands of rDNA loci organized in tandem repeats [12].

Transcriptomics and single-cell sequencing studies across *Plasmodium* species [13,14] have revealed a temporal expression pattern, where the A-type ribosome is dominantly abundant in mammalian parasite stages and the S-type ribosome is dominantly abundant in mosquito parasite stages, while the opposite ribosome type is detected at low levels of abundance. *Plasmodium* ribosomes may also be expressed in two types based on the environmental conditions supporting the development of *Plasmodium* in both a warm-blooded mammal and a

mosquito in ambient temperatures [15]. Given the substantial variation in temperature and nutrient availability between these two host environments, it is plausible – although not confirmed – that the ribosomal structure of *Plasmodium* has undergone specialization to effectively adapt to these distinct parameters. Experimentation conducted by Fang and McCutchan (2016) using different temperatures and nutrients has furthered the assumption that *Plasmodium* A-type and S-type rRNA were responsive to host changes during the malaria life cycle [15].

The A-type and S-type rRNAs maintain different abundance patterns during different stages in the life cycle, as seen in Figure 3. A-type rRNAs have higher abundances during liver and blood stages, whereas S-type remains in low abundance. S-type rRNAs increase in abundance during mosquito stages, becoming most abundant in salivary gland sporozoites, while A-type remains but in low abundance [16]. The sequence heterogeneity and abundance differences between A-type and S-type ribosomes further suggest evidence that *Plasmodium* ribosomes may have a specialized function under different stages in separate host environments.

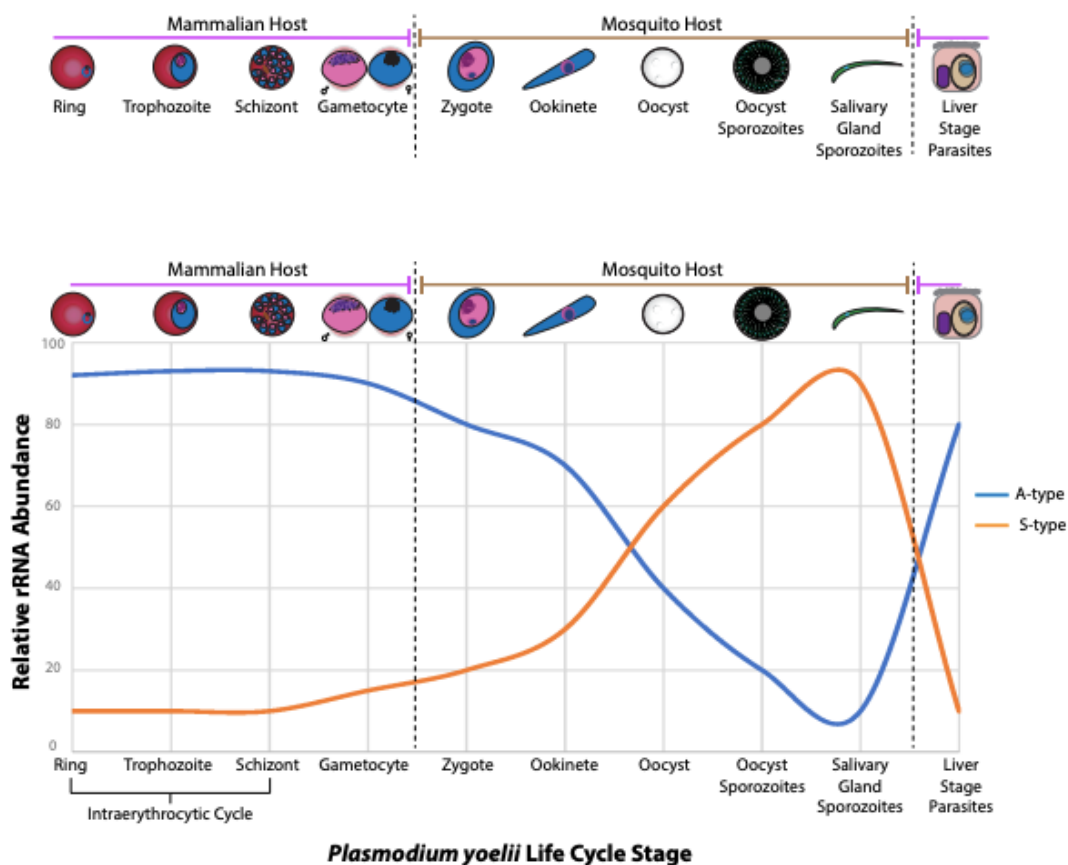


Figure 3. A-Type and S-Type Ribosome Expression throughout *P. yoelii* Life Cycle Stages (McGee, 2019)

1.5 Application of Temporally Expressed Expansion Segments

Plasmodium A-type and S-type rRNAs have sequence variation predominantly located in their expansion segments (ESs), and the variation in nucleotide composition and length results in differing predicted secondary structures [13,16,17]. Seen in Figure 4 is a ChimeraX image of a reconstructed 3-D model of the *Plasmodium falciparum* A-type ribosome determined using previously published structural characterizations [18]. The model illustrates the relative position of where expansion segments are expected to protrude from the rRNA small subunit (SSU) as well as the large subunit (LSU).

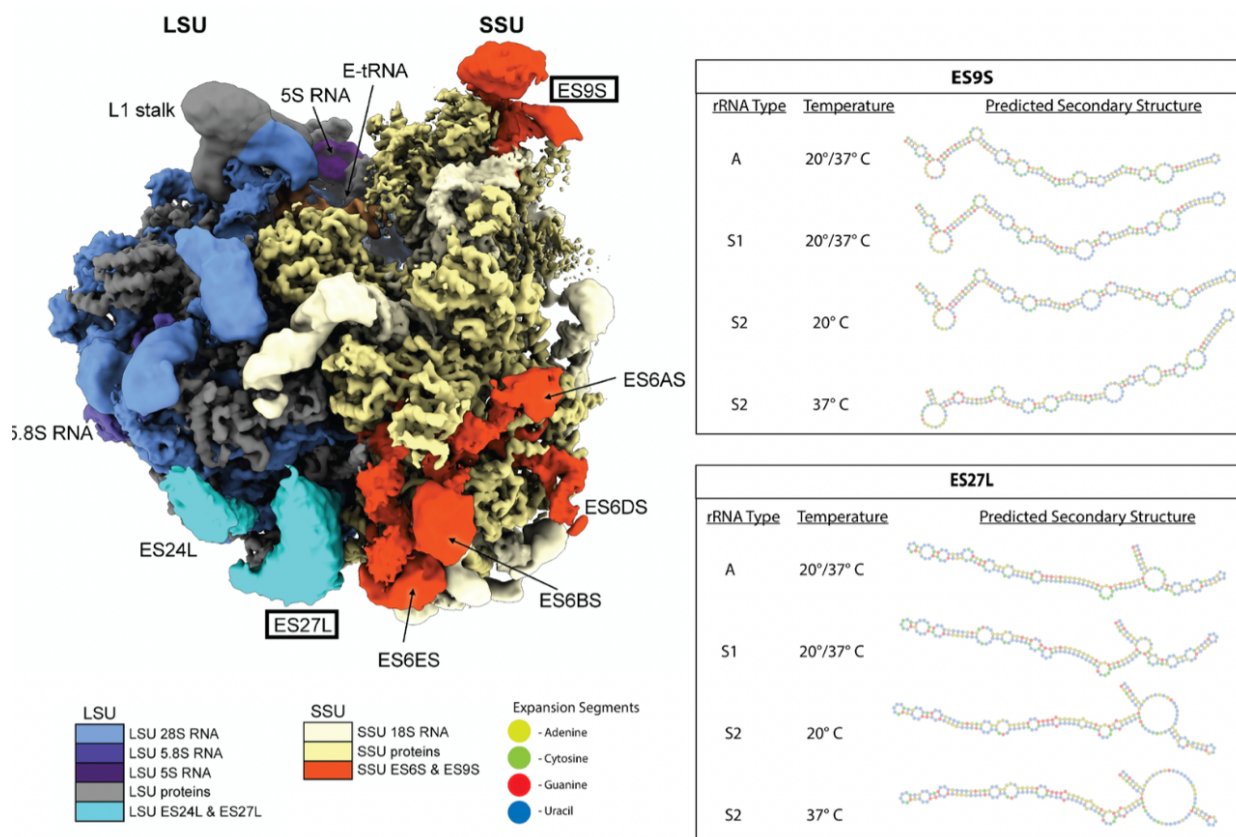


Figure 4. ChimeraX model of *Plasmodium falciparum* A-type Ribosome and Predicted Secondary Structures of A-type and S-type ES9S and ES27L (McGee, 2023)

In Figure 4, it is also seen that the anticipated secondary structures of the two labeled expansion segments focused on in this experiment – ES9S and ES27L – exhibit distinct conformations for A-type or S-type rRNA based on their sequence variation. For example, the rRNA types S1 and S2 observed in Figure 4 exhibit their sequence variations in the 28S gene [19]. Aligning various *P. yoelii* ES sequences across chromosomes 5, 6, and 12 via PlasmoDB also strongly indicates that sequence variation exists amongst A-type and S-type rRNA [20]. These distinctive predicted secondary structures not only highlight the potential importance of the sequence variation existing in these expansion segments, but also begs the question as to why this differentiation exists.

The identified sequence variation, difference in predicted secondary structure, and characterized interaction with ribosome-associated factors led me to want to investigate the potential role of ES9S and ES27L in *Plasmodium* ribosome specialization. Additionally, the observed increase in predicted secondary structure size of ES9S in *Plasmodium*, compared to "humanized" yeast ES9S [10], further suggests a specialized function for the ES that may be essential for the biological requirements of *Plasmodium*.

1.6 Goals and Hypothesis of *Plasmodium yoelii* ES9S and ES27L Experiments

The enigmatically placed expansion segments protruding from *Plasmodium* A-type and S-type ribosomes have long been hypothesized to be specialized, yet specialized function and heterogenous factors contributing to this function have yet to be discovered. The focus of my project was to identify potential specific interactions between selected A-type and S-type ESs and currently unidentified ribosome-associated proteins that could provide specialized functions to specific ribosome types. The objective of this project was to generate a reproducible protocol that allows us to discover if the ESs protruding from rRNA contain variance between the A and S-type sequences utilized by *Plasmodium* ribosomes to recruit specific proteins. Such differences could impact stage-specific translational regulation, indicating *Plasmodium* ribosomes are specialized. With the compelling evidence of rRNA ES interacting with ribosome-associated factors in other eukaryotic organisms, I hypothesized that a subset of the rRNAs that vary between ribosome types will have specific interactions with a protein complex that will play a functional role in the ribosome specialization of *Plasmodium* species. Moreover, identifying proteins that interacted with either A- or S-type ESs will contribute to the overall research gap in this field and would provide a stage-specific ribosome specialization tool that may be absent in

humans and could be potentially targetable to inhibit *Plasmodium* ribosome-specific interactions. For this study, I originally proposed to study two expansion segments – ES9S and ES27L – that have a demonstrated role in ribosome specialization in other species by recruiting specific proteins or messenger RNA

1.7 Experimental Overview

The genome and basic biology of many cellular processes are largely the same between rodent-infectious and human-infectious malaria species, so discovery phase research can be accelerated by using rodent-infectious species such as *P. yoelii*. The Lindner Lab uses the rodent infectious species *P. yoelii* to investigate methods of translational regulation at transmission stages throughout the entire life cycle. To identify specific proteins interacting with the ESs, I used an RNA-centric approach utilizing RNA probes that I would transcribe, purify, and biotin label in the Lindner Laboratory.

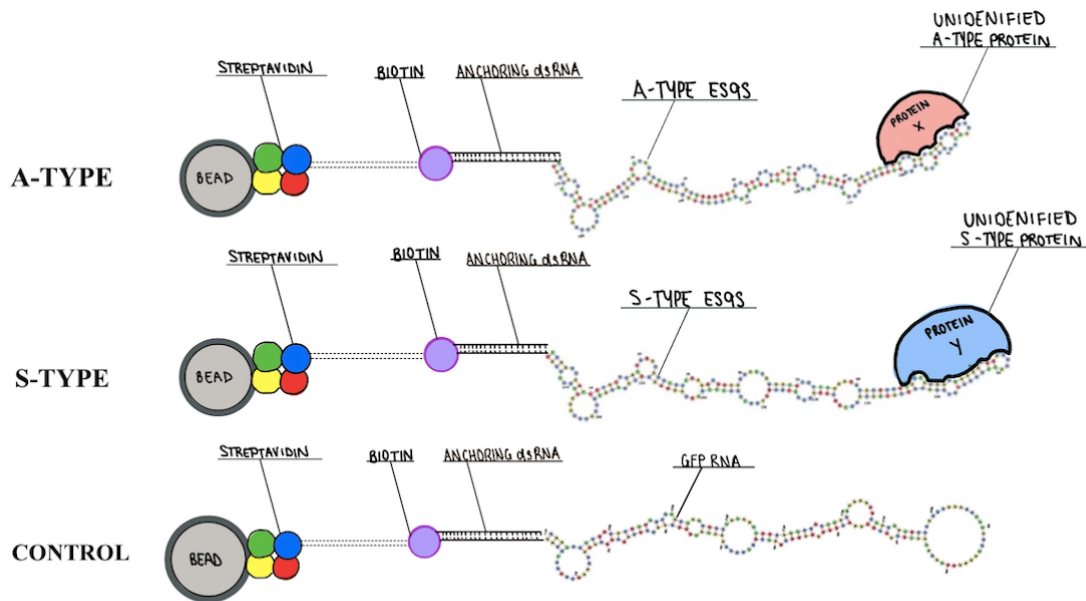


Figure 5. An illustration of ES9S A-Type versus S-Type bound to biotin. The non-covalent interaction between streptavidin is indicated in dashed lines. Proteins X and Y mimic currently unidentified proteins of interest (Wardeh, 2023).

To isolate proteins that bind to a specific ES sequence, I transcribed RNA probes that were to be subsequently biotinylated for capture with streptavidin (SA) conjugated beads using a strong non-covalent interaction between biotin and SA ($K_d = 1 \times 10^{15} \text{ M}$). These specific *P. yoelii* ES sequences, previously determined in the Lindner lab through pairwise sequence alignments to the published sequences of *P. falciparum*, were synthesized and inserted by Twist Bioscience into a synthetic plasmid DNA template containing a T7 promoter. These plasmids were used as the template for a T7 RNA Polymerase (T7RNAP) reaction to produce designated ESs RNAs that were flanked on the 5' and 3' ends with nucleotide sequences and base pair matches to provide a dsRNA structural anchor point [21]. The RNA products were purified using an 8% denaturing polyacrylamide gel. Subsequently, a biotin molecule was added to the RNA using a Poly(A)-tailing reaction with biotin-conjugated substrates. The biotinylated RNA probes were then refolded and allowed to bind with SA on magnetic beads, ultimately generating the probe-bound beads. This interaction between the SA beads and the biotin-bound RNA complex is illustrated in Figure 5. As an example, the ES9S A-Type (top) and ES9S S-Type (middle) expansion segments are conjugated to biotin and interact with SA via non-covalent interactions. To serve as a control ES, a GFP RNA sequence of comparable length (depicted at the bottom) was transcribed. The control GFP ES was created from a BLEB-GFP cell line optimized in *Plasmodium* [22] to determine best practices for the accurate generation of the RNA probes and will be used to control for any non-specific interactions that may occur.

I conducted my workflow optimization efforts by focusing only on generating control ES GFP RNA probes, which mimic the approximate size and predicted structure of the six chosen ES9S and ES27L segments located on Chromosomes 5, 6, and 12 in *P. yoelii*. Generation of the control RNA probe demonstrates I was able to establish a consistent and reproducible procedure

for generating the remainder of the selected ES RNA probes. This standard operating procedure now enables the laboratory to determine whether the selected six ES9S and ES27L A-type and S-type ES sequences selectively recruit proteins, thereby indicating that they may possess specialized translational activity in *Plasmodium*.

Chapter 2

Materials and Methods

2.1 Synthesizing *Plasmodium yoelii* Plasmids

The rDNA loci including the following ES sequences were retrieved from PlasmoDB: *Plasmodium falciparum* A-type ES located on chromosome 7, *Plasmodium yoelii* A-type ES located on chromosome 12, *Plasmodium yoelii* S-type ES located on chromosome 5, and *Plasmodium yoelii* S-type ES located on chromosome 6. ES9S and ES27L secondary structures were identified and annotated using ApE plasmid editor in *Plasmodium falciparum* A-type ES on chromosome 7. The sequences were annotated from *Plasmodium falciparum* 80S ribosome ES secondary structures produced by Wong et al. in 2014 [18]. The annotated *Plasmodium falciparum* chromosome 7 A-type ES sequence was pairwise aligned to Chr 12 A-type *Plasmodium yoelii* rDNA sequence to identify and then annotate the and ES9S and ES27L sequences. The annotated *Plasmodium yoelii* chromosome 12 sequence was pairwise aligned to chromosome 5 and chromosome 6 S-type *Plasmodium yoelii* sequences to identify and annotate the ES9S and ES27L sequences. All annotated sequences were extended by 5 nucleotides to ensure correct secondary structure folding, as these sequences are structured in the cryo-EM structure. A T7 Promoter was added to enable *in vitro* transcription of these RNAs. A START RNA linker and END RNA linker were added, which are 10 base pair sequences that will form a dsRNA helix to anchor the 5' and 3' ends of the ES RNA sequence together (reference figure 5). The designed sequences were then sent to Twist Bioscience, which synthesized, inserted, and sequenced the seven plasmids containing control or experimental ESs.

2.2 Transforming and Purifying Plasmids

NEB5-alpha Competent *E. coli* High Efficiency cells were thawed. Then, 25 μL competent cells were added to 1 μL plasmid in a 1:100 dilution in ddH₂O. Afterward, 7 separate tubes were made with this dilution containing the separately generated ES plasmids. The tubes were labeled as the following: pSL1710 Twist Plasmid Chr5ES9S Seq, pSL1711 Twist Plasmid Chr6ES9S Seq, pSL1712 Twist Plasmid Chr12ES9S Seq, pSL1713 Twist Plasmid Chr5ES27L Seq, pSL1714 Twist Plasmid Chr6ES27L Seq, pSL1715 Twist Plasmid Chr12ES27L Seq, and pSL1716 Twist Plasmid GFP Control Seq. Tubes were incubated on ice for 5 minutes. Tubes were heat-shocked in a hot bath of 42 °C for 30 seconds. The tubes recovered on ice for 5 minutes. The 700 μL of recovery media was added. The tubes were then incubated in a heated bath for 45 minutes at 37 °C. During this time, agar plates treated with ampicillin were warmed to room temperature. Tubes were taken out from the bath and spun down the bacteria in a centrifuge for 3 minutes at 5,000 g. The supernatant was removed, and pellets were resuspended in residual media in each tube. The resuspended pellets were added onto separate agar plates containing 5 glass beads each. Plates were shaken with the beads until the entire agar surface was coated with resuspended pellet. Glass beads were removed from the plates and were incubated at 37°C overnight.

2.3 Picking Colonies

One isolated colony was picked from each plate using a 200 μL pipette tip and incubated in 5ml LB+Ampicillin at 37 °C. The pipette tip was injected into the glass tubes containing the solution mixture, while avoiding touching the sides of the tube so colony only interacted with the

solution. This procedure was repeated for each plasmid plate before putting back into the bacteria warm room overnight. The used plates were sealed and stored face down in the 4 °C fridge for preservation of leftover colonies.

2.4 Plasmid DNA Midiprep

The 100 mL overnight cultures were transferred to 50 mL conical tubes and centrifuged for 10 minutes at 6000 g for the following: pSL1710, 1711, 1712, 1713, 1714, 1715, and 1716. Cell pellets were resuspended in 8 mL of Resuspension (Buffer RES) and added to a 50 mL conical tube. Then, 8 mL of Lysis Buffer (LYS) was added to the suspension, and the tubes were inverted 5 times. The tubes incubated for 5 minutes. Then, 12 mL of Equilibration Buffer (EQU) was added to column filters. All the columns were dampened by slowly adding EQU in a circular motion. Afterwards, 8 mL of Neutralization Buffer (NEU) was added to the suspension and the lysate was mixed by inverting the tubes until the samples were completely opaque. The suspension of the lysate was completely homogenous before adding it to the column filter. Then, the lysate was added to the column filter directly from the falcon tube. The first wash consisted of add 5 mL of Equilibration Buffer in a circular motion to the column filter. The column filters were removed after the first wash. The second wash consisted of adding 8 mL of Wash Buffer (WASH) to the column only. The Plasmid DNA was eluted with 5 ml Elution Buffer (ELU). The eluate was collected in a conical tube.

2.5 Midiprep Finalizer

To begin, 3.5 mL of room-temperature isopropanol was added to each conical tube. The tubes were vortexed well and sat for 2 minutes. The plunger of a 30 mL syringe was removed, and a finalizer was added to the tip of the syringe. The plasmid precipitation mixture was added to the syringe and the plunger was inserted, which allowed precipitate to go through the finalizer drop by drop. After all the precipitate was pushed through, the finalizer and plunger were once again removed. Then, 2 mL of 70% EtOH was added into the syringe along with the finalizer, and the EtOH was pushed out drop by drop via the plunger. The finalizer was dried out six times in a row by removing the finalizer, removing the plunger, and adding the finalizer back, and then pushing the plunger down to remove excess EtOH on a Kimwipe. The finalizer was attached to a 1 mL syringe and 400 μ L of 5 mM Tris (pH 8.0) was added. The eluate was collected in a labeled microcentrifuge tube. The eluate was transferred back into the syringe and eluted into the same collection tube a second time. The eluate was pressed out with air before finishing. This entire procedure was repeated seven times, to purify each midiprep. Each plasmid was assessed by Nanodrop to measure the concentration of plasmid DNA.

2.6 Linearizing ES Plasmids

Each linearization digest began with a microcentrifuge tube containing 50 μ g of midiprep DNA. Then, 60 μ L of 10X CutSmart Buffer was added. Then, 6 μ L of Eco-RI High Fidelity enzyme was added. Each microcentrifuge tube was then filled to 600 μ L with DEPC-treated water after all the other components were added. The digests were incubated at room temperature for 3 hours. To confirm the digests were successful, a 1% agarose gel

electrophoresis was carried out. Then, 5 μL of each digest was put into another tube with 11 μL of DEPC-treated water and 4 μL of 6x loading dye. Afterward, 5 μL of corresponding undigested plasmid was put into a separate tube with 11 μL of DEPC-treated water and 4 μL of 6x loading dye as a negative control. The ethidium bromide-stained gel ran for 30 minutes at 130 volts. The gel was imaged using UV light. After the digests were confirmed to be linearized through gel imaging, the digests were ethanol precipitated. In microcentrifuge tubes, 600 μL of the digest DNA, 60 μL 3M NaOAc, 1200 μL of 100% EtOH, and 1 μL of glycogen were added and mixed thoroughly. The mixture was put into the $-80\text{ }^{\circ}\text{C}$ freezer overnight. Then, the tubes were spun at $4\text{ }^{\circ}\text{C}$ for 10 minutes at 13,000 g. The supernatant was removed without disturbing the white pellet containing the linearized DNA. Next, 500 μL of 70% EtOH was added into each tube, which was then spun at $4\text{ }^{\circ}\text{C}$ for an additional 10 minutes at 13,000 g. The supernatant was again removed, leaving the white pellet to dry at room temperature for 30 minutes. A vacuum was used to dry up the pellet quicker. Each pellet was resuspended in 11 μL of DEPC-treated water. 1 μL of each digest was Nanodropped to record the concentration of plasmid DNA.

2.7 Transcribing Linearized DNA via T7 RNA Polymerase

The New England Biolabs HiScribe T7 High Yield RNA Synthesis Kit was used for transcription of sequences less than 0.3 kb. In PCR tubes, 1 μg of template DNA, 1.5 μL ATP, 1.5 μL GTP, 1.5 μL CTP, 1.5 μL UTP, 1.5 μL T7 RNA Polymerase Mix, and 1.5 μL of 10X Reaction Buffer. The remainder was filled with RNase-free water to have a total reaction volume of 20 μL . Each PCR tube was mixed thoroughly, and pulse spun in the microfuge. The PCR tubes were incubated at $37\text{ }^{\circ}\text{C}$ overnight in a thermocycler.

2.8 Separating ES RNA via 8% SDS Polyacrylamide Gel

This protocol was created and modified by the Lindner Lab with the assistance of Kyle Messina in the Hafenstein lab at Penn State. The following items were gently rinsed with water and wiped off with 70% EtOH: 2 custom-made glass plates, comb with 2 spacers of the same width. The gel plate was set up by inserting spacers between the plates and sealing all sides tightly except the top with electrical tape. The following was combined in 100 mL of H₂O: 2 ml 50X TAE, 20 ml Acryl/Bis 40%, and 48 g Urea. Directly before the gel was poured, 500 μ L APS and 100 μ L TEMED were added. The gel mixture was poured at a 45-degree angle to avoid bubbles. The comb was inserted. The gel was allowed to polymerize upright for 30 minutes. Then, the tape and comb were slowly removed, and the gel plate was positioned on the gel rig in a vertical position, using clips to hold it in place. Black stoppers were added to each side of the point of contact between the plate and gel rig to prevent leaking. 1X TAE was added as a buffer with ethidium bromide to the gel rig until plate wells were fully submerged. The wells were cleaned using a 3 mL needle with TAE buffer before inserting the RNA samples. Then, the RNA samples were denatured by heating at 70 °C on a hot plate for 5 minutes. Afterward, 8 μ L each of 1 bp RNA ladder and RNA sample (2 μ L RNA + 6 μ L formamide + 1.6 μ L 6x loading dye) and a DNA negative control (2 μ L DNA + 6 μ L formamide + 1.6 μ L 6x loading dye) were inserted in their respective wells. The gel ran at 25 Watts for 1 hour. Then, the spacers were removed, and a clean razor blade was used to loosen the sides of the gel before taking apart the gel glass plates. The gel plate was carefully removed from the gel. Plastic wrap was placed on both sides of the loose gel. Buffer and 3 drops of ethidium bromide were added to a plastic container. The gel was placed in a plastic container and put on a shaker for 30 minutes. The gel was removed from shaker and buffer and placed under a UV light. Then, the fluorescent RNA

bands were excised using a clean razor blade and cut into fine pieces before placing them into dialysis tubes for RNA electroelution.

2.9 Extracting and Purifying GFP RNA via Electroelution

For the elution of RNA from the gel slices, 0.3 liters of 0.1X TAE was made. The fine pieces of gel from the SDS PAGE gel were placed in a 3-inch bag of dialysis tubing, which was presoaked with 0.1X TAE for 5 minutes. The bag was sealed with a dialysis clip on one end. A minimal volume of 0.1X TAE was then added to the dialysis bag, where just enough buffer could surround the gel pieces. The bag was sealed on the open end, making sure that all air bubbles were excluded. The horizontal mini-gel apparatus was filled with 0.1X TAE, and placed in the dialysis bag in the apparatus, on the gel platform. The bag was placed so the RNA slice is closest to the negative (black) electrode. Next, 2V/cm was applied to the apparatus and the RNA was set to elute at this potential for 4 hours. The bag was then removed from the gel apparatus, opened carefully on one end, and the buffer (containing the eluted RNA) was recovered with a pipette and placed in an RNase-free microcentrifuge tube. The bag and gel slice were recovered once with 200 μ l of 0.1X TAE to increase recovery substantially. To purify the eluted RNA, 0.1 volumes of 3M Sodium Acetate and 3 volumes of 100% ethanol were added to the microcentrifuge tube. The tube was incubated overnight at -80 °C. The RNA was pelleted by spinning for 30 minutes at 13,000 g at 4 °C. The pellet was washed once with 70% ethanol, the supernatant was removed, and the pellet was then allowed to air dry and resuspended in 21 μ L of RNase-free water.

2.10 Qubit RNA HS Assay

This procedure was adapted from Invitrogen's Qubit™ HS Assay Kit instructions. Only thin-wall, clear 0.5-mL tubes were used for the Qubit™ 4 Fluorometer. Tube lids were labeled "E" for the experimental RNA, "1" for Standard 1, and "2" for Standard 2. The sides of the tubes were not labeled, as this would interfere with the sample read. The Qubit™ working solution was prepared by diluting the Qubit™ RNA HS reagent 1:200 in Qubit™ RNA HS buffer. Qubit™ working solution was added to each tube such that the final volume is 200 μ L. Each standard tube requires 190 μ L of Qubit™ working solution, and each sample tube requires anywhere from 199 μ L of working solution. Then, 10 μ L of each Qubit™ standard was added to its appropriate tube, and 1 μ L of the sample was added into its appropriate tube. The tubes were vigorously vortexed for 5 seconds. All tubes were incubated at room temperature for 2 minutes in a drawer. Then, on the Qubit™ 4 Fluorometer home screen, the RNA button was selected, and RNA High Sensitivity was selected as the assay type. The tube containing Standard #1 was placed into the sample chamber, the lid was closed, and the standard was read. The same steps were followed for Standard #2. The sample RNA tube was then read. On the assay screen, the concentration of RNA was given in μ g/mL. Standard tubes were then discarded.

2.11 Biotin Labeling and Purifying GFP RNA

A PCR tube containing 20 μ L reaction mixtures was created for biotin labeling the purified RNA. Then, 2 μ L of 1M Potassium Acetate, 0.4 μ L of 1M Tris-HCl (pH 8.0), 1 μ L of 40 mM Magnesium Acetate, 1 μ L of 1% NP-40, 2 μ L of 5 mM N6-Biotin-ATP, 1 μ L of *E. coli* Poly(A) Polymerase, and 12.6 μ L of RNA sample (up to 2 mM of RNA could have been used)

were added to the experimental sample PCR tube. For the negative controls that were prepared, one tube contained all the listed compounds besides the N6-Biotin ATP, and another tube contained all the listed compounds besides the *E. coli* Poly(A) Polymerase. These negative controls were created to assess if any background was present when a dot blot was carried out. The PCR tube was placed in a thermocycler for 30 minutes to incubate at 37 °C. To purify the biotinylated RNA, 0.1 volumes of 3M Sodium Acetate and 3 volumes of 100% ethanol were added to the microcentrifuge tube. The tube was incubated at -80 °C overnight. The RNA was pelleted by spinning for 30 minutes at 13,000 g at 4 °C. The pellet was washed once with 70% ethanol, the supernatant was removed, and the pellet was then allowed to air dry and resuspended in 20 µL of RNase-free water.

2.12 Dot Blot Analysis of Biotinylated RNA

A nitrocellulose membrane was cut into four 2-inch pieces for our experimental reaction (Poly(A) Polymerase + Biotin), the positive control (biotinylated *E. coli* RNA), and two negative controls (Poly(A) Polymerase (PAP) with no Biotin, and Biotin with no Poly(A) Polymerase (PAP)). A 3-laned grid was drawn with a pencil to indicate the regions that were going to be blotted. The membranes were soaked in 1X PBS for 10 minutes, and then air dried for 10 minutes on saran wrap in a drawer. Then 0.5 ul, 1 ul, and 2 µL of control sample, experimental sample, and negative control samples were pipetted onto the center of their respective lanes on the nitrocellulose membrane. The area the samples penetrated was minimized by applying the samples slowly using a narrow-mouth pipette tip. The RNA was cross-linked to the membrane at 254 nm wavelength with a UV cross-linker for 1 minute. To ensure the membrane did not dry

out while cross-linking, the membranes were placed on top of a filter paper that had been saturated with 1X PBS. The membranes were incubated in Blocking Buffer (a solution of 125 mM NaCl, 17 mM Na₂HPO₄, 7.3 mM NaH₂PO₄, and 1% w/v Sodium Dodecyl Sulfate in DEPC-treated water) for 30 min while shaking. After incubation, the buffer was discarded. The membrane was incubated with streptavidin-HRP (1:10,000 in Blocking Buffer) for 5 min while shaking. After incubation, the buffer was discarded. The membrane was then washed with Wash Buffer A twice (1:10 dilution of Blocking Buffer in DEPC-treated water) for 20 min while shaking. The buffer was then discarded. The membrane was then washed twice with Wash Buffer B (solution of 100 mM Tris, 100 mM NaCl, 21 mM MgCl₂) for 5 minutes while shaking. The buffer was discarded. The ECL reagent (Thermo Fisher Pierce ECL kit) was made and added to the membrane to incubate for 1 minute. The solution was removed. The membranes were then exposed to UV light and developed as per standard calorimetric and high-resolution laboratory protocols.

2.13 Synthesizing Human Dicer Proteins

The synthesis of the human dicer (hDicer) as a positive control protein was carried out to facilitate the evaluation of its binding affinity towards the RNA probe containing control GFP ES. The hDicer plasmid provided by the Showalter Lab at Penn State was utilized as the template for protein expression. Allen Minns prepared and purified the recombinant protein using *Escherichia coli* and ensured that the quality necessary for the subsequent Electrophoretic Mobility Shift Assay (EMSA) experiment was achieved.

2.14 Protein Binding Confirmation using EMSA

This portion of the protocol was developed and conducted by Allen Minns. To confirm protein binding using an Electrophoretic Mobility Shift Assay (EMSA), a polyacrylamide gel was prepared. The gel mixture comprised 1.2 mL of 5x TBE, 1.8 mL of 40% v/v acrylamide, 120 μ L of 50% v/v glycerol, 8.6 mL of water, 80 μ L of 10% w/v APS, and 20 μ L of TEMED. After thorough mixing, the gel was flushed with 0.5xTBE and pre-run for 35 minutes at 100V, ensuring it was chilled beforehand. While the gel pre-ran, the EMSA samples were prepared. Each 20 μ L reaction included 1 μ L of 100 mM MgCl₂, 1 μ L of 1M KCl, 1 μ L of tRNA (2 mg/mL), 2 μ L of 10x Binding Buffer (comprising 100mM Tris-Cl pH 7.5, 500 mM KCl, 10mM DTT, and water), 1 μ L of biotinylated RNA, 2 μ L of the protein sample, 0.5 μ L of RNase inhibitor, 2 μ L of 50% v/v glycerol, and 9.5 μ L of water. After allowing the samples to incubate at room temperature for 20 minutes, they were applied to the pre-run EMSA gel and electrophoresed for 1 hour at 100V in chilled 0.5xTBE. For the transfer, powder-free gloves and new sponges were used. Nylon membrane and four pieces of filter paper were soaked in 0.5xTBE, stacked in the cassette with the EMSA gel between the membrane and filter paper layers, and then clamped together. The cassette was placed into the gel running tank, filled with pre-chilled 0.5xTBE, and run for 1 hour at 380 mM. Following electrophoresis, cross-linking was conducted using the Stratalinker with the auto-crosslink setting applied twice. Subsequently, the dot blot protocol from Section 2.7 for RNA labeling verification was employed to complete the protein binding confirmation process.

Chapter 3

Results

3.1 Verification of Transforming and Transcribing ES DNA

The six chosen ES9S and ES27L DNA sequences from A and S-type rDNA loci and the GFP control sequence were designed and sent to Twist Bioscience for synthesis, plasmid insertion, and sequence validation in accordance with Table 1.

Table 1. The selected *Plasmodium yoelii* ES DNA Sequences on Chromosomes 5, 6, 12, and Control GFP.

Each sequence, sent to Twist Bioscience for *generation*, was identified by its chromosome location and ES type, along with its corresponding plasmid designation label (pSL) and size in kilobases (kb). The DNA strand is highlighted in magenta, while the 21 bp linker sequences, facilitating the non-covalent interaction between the RNA and biotin, are highlighted in yellow. Each sequence contained a GAATTC sequence allowing for Eco-RI restriction enzyme cleaving.

Yellow Highlight: LINKER

Magenta Highlight: ES

Sequence Name	Sequence Nucleotides (from 5' to 3')	Size (kb)
PYChr12A-Type ES9S: (pSL 1710)	AACCTGCTAA TTAGCGGCGAGTACGCTATATCCTTTATCGG GGGATTGGTTTTGACGTTTTTGCGGTCATACTGCTTAATCAA TTGGTTTACCTTTTGCTCTTTGCGGTATGTTTCTCGCATCTT CGACATGCCTCTCTTGATAAGGATGTATTCGCTTTATTTA ATGCTTC TTAGAGGAAC	.186 kb
PYChr12A-Type ES27L (pSL 1711)	CTGAGGACATATGAGTAGAGCAGTTTAAATTAACGTTTGAA AAATGATTTAAAGAAAGCACCTTGGTTCGCCATCGTGT TATTTTATTTTCGTTTATCTCATGTTTATTTTATTCTATCCCTC TACTCGCCGCTATTTTAAACGTCACCTTCGGTGGCGTTTTATG GCATTATCA TGTAACTCA	.186 kb
PYChr5S- Type ES9S: (pSL 1712)	AACCTGCTAA TTAGCGGCGAGTACGCTATATCCTTTATCGG GGGATTGGTTTTGACGTTTATGCGGTCATACTGCTTAATCA ATTGGTTTACCTTTTGCTCTTTGCGGTATGTTTCTCGCATCT TCGACATGCCTCTCTTGATAAGGATGTATTCGCTTTATTT AATGCTTC TTAGAGGAAC	.185 kb
PYChr5S-TypeES27L: (pSL 1713)	CAAGGAGTCTAACAAATGTGCGAGCGTATATATGTTTTAAC TATTAATAAAAAGAAACATTTCAACCTTTTATAATACGCGTA ATTAAAGTGTAAGAGCTTAACCTTTTGTAGAACATACTAG ATTGATCCATTATATTTTACAGTGGCGACTGAAAAATAATG TGCTTCAGTTAAGTATATGCATACAGATCCCGTTGACAAA CGTCAAACCGAGAGTGAGTATATTTGTTAGGACCCGAGAG GCTTTGAACCTAAGCGTGGTGAGATTGAAGTCGGGTGAAAG CCTGATGG	.293 kb
PYChr6S-TypeES9S: (pSL 1714)	AACCTGCTAA TTAGCGGTAGTTACGTGATATTCTTCGAAGT GGAATTAATAACGTTTCCAAAGTTATGTTGCATCATAAT CAAAATGGATTTACCTTTTGTATTATTGTAGCATATTCGGTG	.188 kb

	GATTCGTTGGATTCTTCCCTAGTAAGGATGTATCTACTTT ATTTAAAGCTTCTTAGAGGAAC	
PYChr6S-TypeES27L: (pSL 1715)	CAAGGAGTCTAACAAATGTGCGAGCGTATGTATGTTTTTAA CTATATTCTTAATGTTTACGCGTAATTAATGTATCAGAATCT TATGTAGATTGTACTGATGGATAATGTTTATTATTCATTGGA AGTACATGCACACAATACCGGTTAGCAATTACGCTTAATTG AGTATGAGTATATTTGTTAGGACCCGAGAGGCTTTGAACTA AGCGTGGTGAGATTGAAGTCAGACGAAAGTCTGATGG	.244 kb
Control GFP: (pSL 1716)	AATTCCTGTTGAATTAGATGGTGTGTTAATGGGCACAAAT TTCTGTCAGTGGAGAGGGTGAAGGTGATGCAACATACGG AAAACCTACCCTTAAATTTATTTGCACTACTGGAAAACACTAC CTGTTCCATGGCCAACACTTGTCACTACTTTCGCGTATGGTC TTCAAT	.17 kb

Plasmids were successfully transformed into *E. coli* and were selected using ampicillin-resistant agar plates. Following growth in LB media with ampicillin, midi preps were performed to isolate and purify the DNA before linearization. The use of finalizers to purify the midi preps was successful, and the plasmid eluate was collected for linearization.

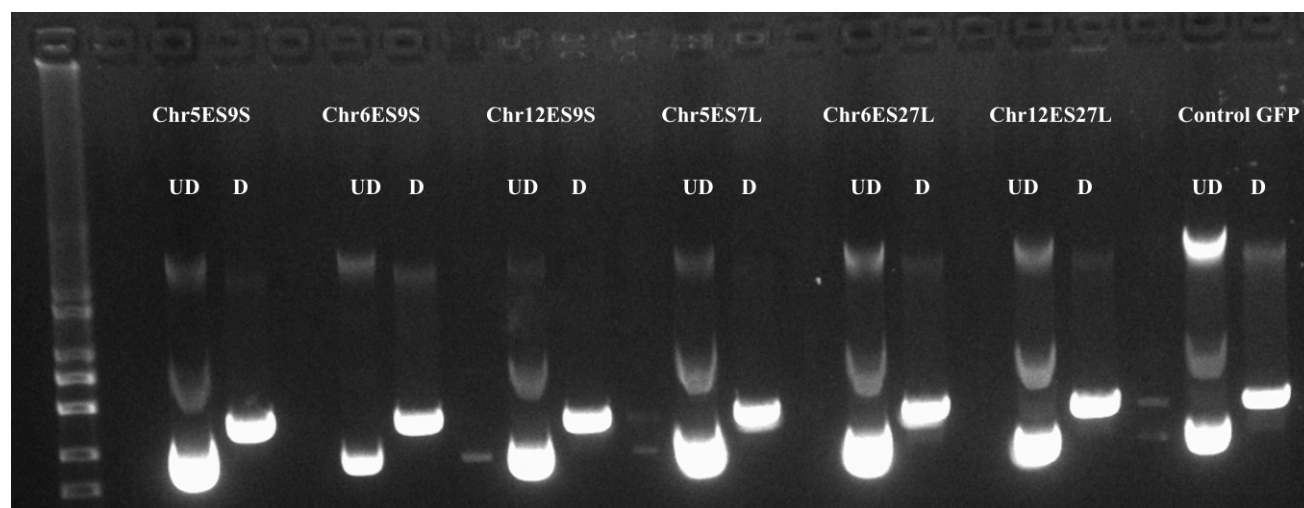


Figure 6. 1% Agarose Gel Confirming Linearization of Selected ES9S and ES27L Plasmid DNA

As seen in Figure 6, the linearization for all chosen ES plasmids was successful, as evidenced by the agarose gel electrophoresis results. Digested ES DNA samples – denoted as "D" - exhibited a distinct migration pattern around 2 kb, appearing to be linearized compared to

their undigested – denoted as "UD" – counterparts, which ran near 3 kb. This difference in migration indicates successful linearization, as the undigested DNA, being supercoiled, migrated further along the gel. These results confirm the efficacy of the linearization procedure that was employed.

Nanodrop data analysis was conducted to quantify the plasmid DNA for each sequence, confirming that sufficient amounts after ethanol precipitation were obtained for transcription into ES RNA, as seen in Table 2.

Table 2. Concentrations of *Plasmodium yoelii* Expansion Segment (ES) linearized DNA.

The table presents the results of Nanodrop data analysis, indicating the concentration of each ES DNA plasmid in nanograms per microliter (ng/ μ l). It should be noted that Nanodrop measurements can become slightly inaccurate after surpassing 2000 ng/ μ l. However, this nanodrop analysis was conducted primarily to determine if the concentration reached or exceeded this threshold for further experimentation.

Expansion Segment Name	Concentration (ng/μL)
PYChr12A-Type ES9S	4110.7
PYChr12A-Type ES27L	3459.0
PYChr5S-Type ES9S	2699.9
PYChr5S-TypeES27L	3917.0
PYChr6S-TypeES9S	3829.8
PYChr6S-TypeES27L	5290.3
Control GFP	4395.0

3.2 Confirmation of the Production and Purification of ES RNA

The T7 RNA transcription reaction of the selected ES DNA sequences into double-stranded RNA sequences was monitored through analysis on an 8% SDS polyacrylamide gel. Notably, the RNA molecules exhibited significantly faster migration compared to DNA molecules, with sizes ranging from 170 to 400 base pairs (see Table 1 sequence sizes), whereas the DNA fragments were approximately 2 kilobases in length. Despite the smearing of RNA bands observed on the gel, attributable to the high amount of RNA synthesized in this

transcription reaction, the distinct separation of RNA from DNA at the top of the gel or embedded within it was evident upon UV light imaging (see Figure 7). This distinct difference in migration patterns and the visual separation of RNA and DNA validate the efficacy of the T7 RNA transcription process employed in this study.

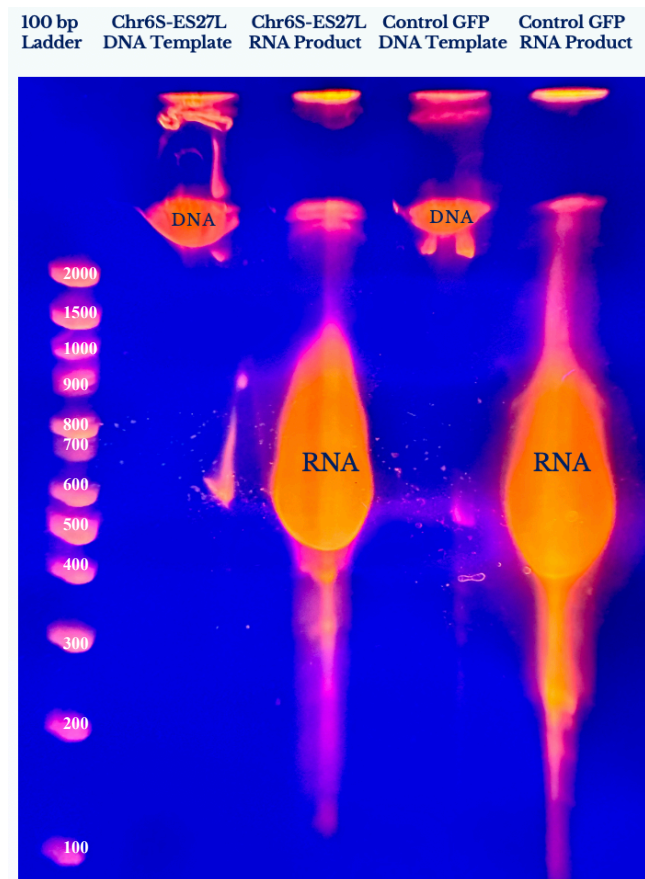


Figure 7. Confirmation of Transcribing ES RNA from ES DNA using Chr6S-ES27L and Control GFP DNA Templates using an 8% SDS Polyacrylamide Gel

For the 8% polyacrylamide gel analysis, only Chr6S-ES27L and Control GFP RNA (and their respective DNA templates from linearization) were selected for comparison. The decision to include these specific samples was based on the expectation that the Control GFP RNA would migrate slightly longer than Chr6S-ES27L due to its smaller size. This anticipated result is

reflected in our data in Figure 7, where Chr6S-ES27L RNA migrated less than Control GFP RNA. This selection aimed to facilitate clearer visualization and comparison of the RNA products synthesized from both DNA samples. Notably, the RNA smear produced by Chr6S-ES27L extended to the end of the gel in its respective lane, confirming the selection of Control GFP RNA as a reference for distinguishing migration patterns. The RNA smears observed in Figure 7 were applicable to this study and attributed to the large concentration (up to 180 μg) of RNA loaded into the wells, resulting in a slower migration of RNA. However, DNA bands are still clearly distinguished from the RNA smears. The RNA smears were excised for electroelution in addition to the RNA that traveled the full length of the gel.

Electroelution was successfully performed, and subsequent ethanol purification of the 30 μL of eluate collected from the dialysis tubes was also successful. These preparatory steps were conducted in anticipation of further qubit analysis, aimed at quantifying the RNA concentration accurately. The Qubit HS RNA assay analysis revealed approximately 24 $\mu\text{g}/\text{mL}$ of Chr6S-ES27L RNA in a 30 μL sample, equating to 7.2 μg of purified 1715 RNA. Additionally, the analysis indicated around 50 $\mu\text{g}/\text{mL}$ of control GFP ES RNA in the same volume, translating to 15 μg of purified control GFP RNA. It's worth noting that the target for binding to streptavidin beads is 20 μg to saturate 100 μL of beads. Given, the preliminary nature of this experiment, I proceeded with the available quantities for biotinylation. Furthermore, for subsequent experiments in developing this protocol, only control GFP ES RNA was utilized as it is expected that all RNAs will behave similarly in an optimized protocol.

3.3 Confirmation of Biotinylating ES RNA

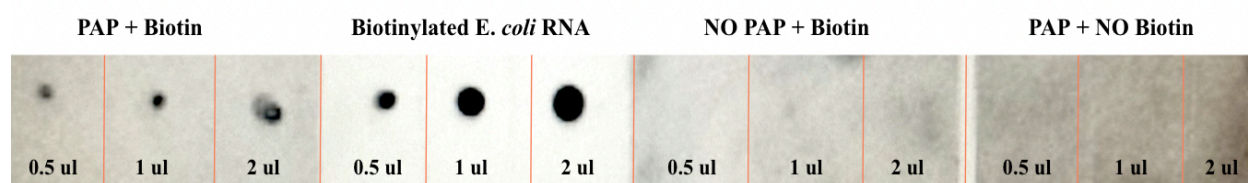


Figure 8. Confirmation of Biotinylated Control GFP ES dsRNA using Dot Blot Analysis

The Dot Blot analysis in Figure 8 serves as a validation for the detection of biotin and efficiency of the biotinylation protocol applied to control GFP ES dsRNA using Poly(A) Polymerase (PAP) and N6-Biotin-ATP. The presence of the discernible dark spots on the control GFP ES dsRNA blot denoted as PAP + Biotin are analogous to those observed in the positive control representing biotinylated *E. coli* RNA, which provides evidence of the success of both biotinylation and dot blot procedures. Notably, the absence of dark spots in the negative control images - noted as NO PAP+ Biotin and PAP + NO biotin - negates the possibility of background interference and reinforces the conclusion that the observed dots indicate biotinylated dsRNA.

3.4 Confirmation of ES RNA Binding to Proteins

The purpose of selecting Human Dicer (hDicer) protein is to use it as a spike-in positive control to ensure the binding of this protein to our ES RNA probe in future proteomics steps. As characterized by the Showalter Lab at Penn State, hDicer is known to bind to dsRNA strands down to 12 base pairs long [23]. Therefore, hDicer could bind to the 21 base pair dsRNA designed as anchoring helices on our ES RNA probes. The hDicer protein plasmid obtained from the Showalter Lab was cultured in *Escherichia coli* BL21 strain and was subsequently expressed and purified to a high degree of purity by Allen Minns prior to the Electrophoretic Mobility Shift

Assay (EMSA) analysis. This ensured the availability of a reliable and concentrated source of a positive control protein for the experimental investigation into its binding affinity with biotinylated control GFP dsRNA.

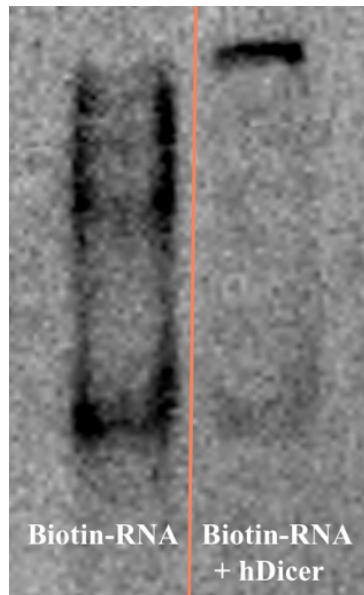


Figure 9. Confirmation of Human Dicer Protein binding to Biotinylated Control GFP ES dsRNA using EMSA

The Electrophoretic Mobility Shift Assay (EMSA) protocol was successfully executed by Allen Minns to assess the binding of Human Dicer protein (hDicer) to the biotinylated control GFP dsRNA constructs. Figure 9 illustrates the hDicer binding interaction with the dsRNA portion of the RNA probe that was introduced via complementary sequences at the 5' and 3' ends of all probes, as evidenced by a noticeable upward shift observed in the Biotin-RNA + hDicer lane compared to a sample lacking hDicer. This shift confirms the functionality of hDicer in binding to the biotinylated dsRNA molecules to serve as a positive control in this study, by ensuring that the generated probes are capable of recruiting proteins. The functionality of hDicer in this experiment allows us to use the protein as a spike-in control to optimize future proteomics procedures, such as mass spectrometry, which would be used to identify and characterize novel proteins that are selectively recruited to the seven selected ES probes. It is important to note that

while hDicer demonstrates binding activity down to 12 base pairs (bp) and accommodates larger structures such as the 21-bp linker helices on control GFP dsRNA, it also exhibits a preference for binding to 16-bp dsRNA structures [23].

Chapter 4

Discussion

4.1 The established methodology for generating ES probes is reproducible and effective

The protocol outlined in Chapter 2 for generating ES probes was successful and reproducible, which enables its use for the generation of RNA probes in future experiments. The initial selection of six expansion segments from chromosomes 5, 6, and 12, focusing on ES9S and ES27L, were chosen due to their documented ability to recruit specific protein complexes in other eukaryotes [8,10]. Notably, the ES9S sequences in *Plasmodium* are extended compared to other eukaryotes, hinting at potential specialized functions, particularly within A and S-type ribosomes [18]. While time constraints limited the comprehensive testing of all selected ESs, the control GFP ES was chosen as a viable model during the preliminary protocol development phase. Nonetheless, replicating the protocol with the chosen ESs remains a priority for future investigations.

During the experimentation process, transcribing linearized DNA via T7 RNA polymerase was highly successful, resulting in a high yield of RNA as seen in Figure 7. However, purifying the resulting RNA product presented challenges. Treating the T7 RNA polymerase product with DNase - a traditional RNA purification method that removes plasmid DNA from RNA products - would remove DNA contamination but would not remove potential RNA contamination such as the RNA products produced at incorrect lengths. To address this, a gel protocol was developed to visualize and quantify only the ES RNA sizes of interest. Despite the time constraints of this project, a protocol for preparing ES RNA via 8% SDS polyacrylamide gel and subsequent electroelution was optimized. Identifying the correct

polyacrylamide gel concentration was crucial for effectively separating the RNA and DNA of interest. However, the encasement of the ES RNA in the gel posed challenges. I overcame these challenges by performing the necessary excision and electroelution procedures. However, this resulted in the loss of a significant portion of viable RNA. Scaling up the number of gels used for each ES RNA sequence is imperative, or switching to a different purification approach will be needed to meet the required RNA concentration for subsequent protocols.

The biotin labeling and purification of GFP dsRNA was successful, as determined by the clear biotin labeling observed in the experimental dot blot compared to the negative and positive control samples. The dot blot served as an effective validation tool, offering visual confirmation of successful biotinylation via N6-Biotin-ATP and Poly(A) Polymerase. Although the biotinylation was successful per dot blot analysis, it is essential to next determine the quantity of RNA that was successfully biotinylated in future experiments. Quantifying the amount of biotinylated RNA would provide valuable information on the efficiency of the labeling process outlined in Chapter 2. For example, if only a small amount of RNA was successfully biotinylated, then the strength of the future steps, such as binding the biotinylated RNA to streptavidin beads, would be severely affected as streptavidin relies on a minimal concentration of biotinylated RNA to bind successfully. Overall, quantifying the amount of biotinylated RNA would allow for proper planning and execution of downstream applications and experimental outcomes, so optimizing this labeling protocol would lead to a more robust preparation of SA beads bound to the RNA probes to ensure efficient, reproducible, and high-quality results in future experiments.

4.2 Successfully establishing a preliminary protocol with GFP ES RNA

The utilization and focus on the control GFP ES to generate the preliminary experimental protocol allowed for meticulous verification of the protocol's reproducibility, ensuring that the techniques employed are reliable and reproducible. The similarity in size and approximate structure between the GFP sequence and the selected ES9S and ES27L sequences enhanced the protocol's applicability to the specific ESs of interest within the *Plasmodium* ribosomal genome.

Using the control GFP sequence to ensure each method within the developed protocol was successful not only improved the credibility of the outlined research methods but also instilled reliability for the subsequent application of the protocol to the previously selected ES9S and ES27L sequences. As such, the reproducibility of the protocol, confirmed through the GFP control experiment, provides a solid foundation for the successful generation of ES9S and ES27L probes tailored to the selected regions on chromosomes 5, 6, and 12 of *Plasmodium yoelii*. Essentially, developing a protocol for creating ES probes in *Plasmodium yoelii* allows us to model the function of ESs protruding from A and S-type ribosomes in human-infectious species such as *Plasmodium falciparum* and determine if they recruit temporally expressed proteins.

4.3 hDicer as a positive control spike-in protein for future proteomics

The RNA-binding affinity of hDicer protein to biotinylated control GFP ES dsRNA holds significant value for the development of ES9S and ES27L RNA probes capable of binding novel protein complexes. Given that the control GFP ES was chosen to develop the preliminary protocol, it was essential to use hDicer as a positive control to validate if the probes could harbor RNA-protein interactions. To address this need, we turned to the research conducted by Scott

Showalter's lab at Penn State, who determined the structure of the double-stranded RNA-binding domain (dsRBD) of hDicer [23]. The ability of hDicer to bind to the dsRNA linker will serve as a positive control to detect if our probes are interacting with other undetermined proteins. Moreover, incubating ES probes with a parasite lysate-hDicer mixture will enhance the reliability of future proteomics. Using the presence of hDicer in proteomics data as a positive control ensures proteins can bind to the probe and will also detect the quantity of probes present in the data based on the quantity of attached hDicer. Using hDicer for quantifying probes will improve the accuracy of our data while also identifying specific interactions that result in variations in proteomics data compared to positive control data.

Human Dicer was successfully prepared in *Escherichia coli* by Allen Minns and incubated with the biotinylated control GFP ES dsRNA to confirm the probe's efficacy. This binding interaction was verified by Allen Minns using electrophoretic mobility shift assay (EMSA), a technique commonly used to detect protein-nucleic acid interactions. In EMSA, the upward shift in electrophoretic mobility indicates the formation of protein-RNA complexes. In Figure 9, a clear upward shift was observed, demonstrating that hDicer is functional and capable of binding to the dsRNA anchoring sequences near the 5' and 3' ends of our biotinylated dsRNA molecules. This successful interaction confirms the functionality of hDicer as a positive control protein and validates the efficacy of the RNA-protein interactions on the ES probes. Overall, the ability of hDicer protein to bind to biotinylated dsRNA molecules provides confidence in the functionality of our ES RNA probes to interact with protein and protein complexes and in distinguishing non-specific interactions, which allows for future characterization of novel proteins selectively recruited to specific ES sites.

4.4 Future Directions for Generating ES Probes

There are several directions that could be taken to advance the outlined protocol for generating *Plasmodium* ES probes. Due to the time constraints of this project, several key procedures remain to be optimized. Firstly, scaling up the reaction to include the remaining six ES9S and ES27L sequences originally selected would allow for investigation into specific ES protein-RNA interactions using proteomics with the hDicer protein as a positive control to confirm probe-protein interactions, quantify results, and separate specific and non-specific interactions.

Additionally, conducting the streptavidin (SA) binding protocol, which was not feasible within the timeframe of this study, would allow for a strong non-covalent bond between biotin and streptavidin. Binding the probes to SA would demonstrate these probes can be bound to SA beads, which would be the reagent necessary to ultimately perform the experiment to pull out ES RNA interacting protein from parasite lysate. Furthermore, troubleshooting with alternative methods for probe generation may be necessary to overcome technical challenges encountered during further protocol developments.

4.4.1 Incorporating the streptavidin binding protocol into biotinylated ES dsRNA probes

Incorporating the streptavidin binding – as commonly performed in the Lindner Lab - after creating biotinylated ES dsRNA probes holds significant promise for enhancing the specificity and efficiency of novel RNA-protein interactions in *Plasmodium* A or S-type ribosomes. While biotinylation of RNA probes allows for precise tagging of target RNA molecules, streptavidin-coated beads offer a solution for capturing and isolating RNA probes that

recruit protein complexes. Streptavidin, with its exceptionally high affinity for biotin ($K_d = 1 \times 10^{15} \text{ M}$), forms a stable complex that can withstand harsh washing conditions, making it ideal for capturing RNA molecules from complex samples such as *Plasmodium yoelii* lysate. By utilizing streptavidin-coated beads as a step after confirming that RNA was biotinylated using a dot blot, we can efficiently purify biotinylated RNA probes, enabling downstream proteomics applications, such as mass spectrometry, to identify and quantify novel proteins bound to the ES probes based on their mass-to-charge ratio.

Although the RNA probes have been successfully biotinylated in this study, the incorporation of the streptavidin binding protocol was not performed due to time constraints. Instead, an electrophoretic mobility shift assay (EMSA) was employed to demonstrate that protein capture is possible using hDicer as a positive control model system. However, the SA binding protocol is essential for future experiments involving the incubation of biotinylated RNA probes in *P. yoelii* lysate. By implementing streptavidin binding, future experiments can efficiently pull out specific protein complexes associated with the biotinylated RNA probes, shedding light on the intricate RNA-protein interactions within *Plasmodium* ESs and advancing our understanding of their translational specialization.

4.4.2 Utilizing Plasmodium yoelii Parasite Lysate

In future studies, using a *Plasmodium yoelii* parasite lysate and hDicer protein mixture to incubate *Plasmodium* ES9S and ES27L probes offers several advantages for identifying the recruitment of specialized proteins. Firstly, the parasite lysate provides a physiologically relevant environment for the probes by containing a complex mixture of proteins that closely mimic the

cellular environment of the parasite, thus ensuring an accurate representation of *in vivo* conditions. Additionally, the assortment of proteins present in the parasite lysate allows for the exploration and proteomics analysis of a wide range of potential protein interactions, therefore enhancing our understanding of the mechanisms underlying translational regulation and other essential processes within *Plasmodium*. Using a mixture of parasite lysate spiked with hDicer protein will also provide all ES probes with a positive control to assess the quantity of probe-protein interaction, the ability of the probes to bind protein, and for non-specific interactions.

P. yoelii blood-stage parasite lysate should be used because the Lindner Lab has recently observed that contrary to the literature, the S-type rRNAs are expressed in these stages at low levels, and yet still play a functional and potentially specialized role in blood-stage infection to enable an early phase of transmissibility to mosquitoes (personal communication, James McGee and Scott Lindner). For future studies, *Plasmodium yoelii* lysate should be generated from Py17XNL (WT) strain parasites grown *in vivo* within 6 to 8-week-old Swiss Webster Mice. The parasitemia of infected mice can be monitored by blood smears stained with Giemsa, and upon parasitemia (percent of parasitic RBCs) reaching 2-3%, infected blood can be collected from euthanized mice following IACUC-approved protocols. Parasite cells can be disrupted to extract material physically using sonication and Dounce homogenization in a lysis buffer containing gentle, non-ionic detergents (e.g., NP-40), protease inhibitors to prevent parasite protease activity, and RNase inhibitors to prevent RNA degradation and ensure the highest yield of isolated proteins. The lysate from this procedure, along with hDicer, will be incubated with SA beads bound with the RNA segment of interest.

4.4.3 Potential Pitfalls and Alternate Approaches

It is plausible for the preliminary protocol proposed to be unsuccessful at identifying RNA-protein interaction, as would be observed by an absence of novel proteins recruited to all six *P. yoelii* ES probes. This absence of specifically associated proteins detected in ES9S or ES27L probes when incubated in parasite lysate would present a challenge in identifying and distinguishing potential protein-RNA interactions. To overcome this limitation, I propose the utilization of a formaldehyde cross-linking procedure. This method involves chemically linking proteins to RNA via covalent bonds, thereby stabilizing protein interactions with the ES sequences. The cross-linking process not only prevents protein dissociation during subsequent washing steps but also enables stringent wash conditions. These stringent wash steps are essential for removing additional contaminants while retaining specific protein-RNA interactions, thus enhancing the reliability and accuracy of our findings.

In cases where there is an insufficient yield of the protein of interest, adjustments to the preliminary protocol become necessary to optimize protein retrieval and stringency. Specifically, the amount of RNA-bound beads used in the experiment can be modified and wash conditions can be adjusted accordingly. Increasing the number of RNA-bound beads can potentially capture more of the protein of interest from the lysate. Meanwhile, fine-tuning the wash conditions, such as altering the buffer composition or incubation time, will allow for a balance between maximizing protein recovery and maintaining stringent washing to eliminate non-specific binding molecules. These adjustments are crucial for ensuring the success of the experimental protocol and obtaining reliable data for subsequent analyses.

4.5 Summary

For decades, understanding the role of ESs in translational control and their varying significance across species has remained a mystery. This knowledge gap hinders our knowledge regarding ribosomal specialization and translational regulation in *Plasmodium* species. Therefore, ribosomal biology - including the exploration of expansion segments - continues to be an active area of research. Developing a reproducible and robust protocol for creating ES probes tailored to *Plasmodium* is essential, given the critical roles these segments could play in the parasite's translational machinery. Experimentation with these conserved ES regions is important for exploring ribosomal specialization within the parasite, making them prime targets for investigation. Understanding how novel proteins are recruited to the A- or S-type ribosomes via these ES segments is crucial for understanding the regulatory networks governing translational control in *Plasmodium*. Furthermore, proposing a technique to explore ES RNA-protein interactions could be a step forward in research of eukaryotic specialized ribosomes. This method could thereby partly be responsible for understanding other specific eukaryotic RNA-protein interactions and the conservation of fundamental molecular mechanisms inherited by different living organisms. Moreover, this method could be useful in other biological systems, such as in zebrafish, where there are multiple ribosomal RNA types [24]. This extended applicability on the potential of this research method in discovering fundamental principles associated with specific RNA-protein interactions and their regulational role in various biological processes.

By establishing a reproducible protocol for generating ES probes to further our understanding of *Plasmodium's* translational machinery, we take a significant stride toward advancing the field of ribosomal biology. Ultimately, advancements in our understanding of

Plasmodium translational regulation offers hope for the development of drugs that target molecular complexes produced at specific stages of the parasite's development to prevent malaria transmission.

BIBLIOGRAPHY

1. World Health Organization. (2022). World Malaria Report 2022.
<https://www.who.int/teams/global-malaria-programme/reports/world-malaria-report-2022>
2. Center for Disease Control and Prevention. (2022). Drug Resistance in the Malaria-Endemic World.
https://www.cdc.gov/malaria/malaria_worldwide/reduction/drug_resistance.html
3. Alven, S., Aderibigbe, B.. (2019). Combination Therapy Strategies for the Treatment of Malaria. *Molecules*. 24(19). <https://doi.org/10.3390/molecules2419360>
4. Norris, K., Hopes, T., & Aspden, J. L. (2021). Ribosome heterogeneity and specialization in development. *Wiley Interdisciplinary Reviews. RNA*, 12(4).
<https://doi.org/10.1002/wrna.1644>
5. McGee, J., Armache, J-P., Lindner, S.. (2023). Ribosome heterogeneity and specialization of *Plasmodium* parasites. *PLoS Pathog* 19(4).
<https://doi.org/10.1371/journal.ppat.1011267>
6. Gerbi, S.A. (1986). The evolution of eukaryotic ribosomal DNA. *Biosystems*, 19(4), 247-258. [https://doi.org/10.1016/0303-2647\(86\)90001-8](https://doi.org/10.1016/0303-2647(86)90001-8)
7. Ramesh, M.W. (2016). Eukaryote-specific rRNA expansion segments function in ribosome biogenesis. *RNA*, 22(8). <https://doi.org/10.1261/rna.056705.116>
8. Fujii, K., Susanto, T., Saurabh, S., Barna, M.. (2018). Decoding the Function of Expansion Segments in Ribosomes. *Molecular Cell*, 72(6), 1013-1020.
<https://doi.org/10.1016/j.molcel.2018.11.023>

9. Genuth, N. R., & Barna, M. (2018). The Discovery of Ribosome Heterogeneity and Its Implications for Gene Regulation and Organismal Life. *Molecular cell*, 71(3), 364–374. <https://doi.org/10.1016/j.molcel.2018.07.018>
10. Leppek, K., Fujii, K., Quade, N., Susanto, T., Boehringer, D., Lenarčič, T., Xue, S., Genuth, R., Ban, N., Barna, M.. (2020). Gene- and Species-Specific Hox mRNA Translation by Ribosome Expansion Segments. *Molecular Cell*, 80(6), 980-995. <https://doi.org/10.1016/j.molcel.2020.10.023>
11. Thompson, J., van Spaendonk, R. M., Choudhuri, R., Sinden, R. E., Janse, C. J., & Waters, A. P. (1999). Heterogeneous ribosome populations are present in *Plasmodium berghei* during development in its vector. *Molecular Microbiology*, 31(1), 253–260. <https://doi.org/10.1046/j.1365-2958.1999.01167>.
12. Potapova, T. A., & Gerton, J. L. (2019). Ribosomal DNA and the nucleolus in the context of genome organization. *Chromosome Research*, 27(2), 109–127. <https://doi.org/10.1007/s10577-018-9600-5>
13. Gunderson, J. H., Sogin, M. L., Wollett, G., Hollingdale, M., de la Cruz, V. F., Waters, A. P., et al. (1987). Structurally distinct, stage-specific ribosomes occur in *Plasmodium*. *Science*, 238(4829), 933–937. <https://doi.org/10.1126/science.3672135>
14. Fang, J., Sullivan, M., & McCutchan, T. F. (2004). The effects of glucose concentration on the reciprocal regulation of rRNA promoters in *Plasmodium falciparum*. *Journal of Biological Chemistry*, 279(1), 720–725. <https://doi.org/10.1074/jbc.M310168200>
15. Fang J., McCutchan T.F.. (2016) Corrigendum: Malaria: Thermoregulation in a parasite's life cycle. *Nature*, 537(7619) <https://doi.org/10.1038/nature18931>

16. Qi, Y., Zhu, F., Eastman, R.T., Fu, Y., Zilversmit, M., Pattaradilokrat, S., Hong, L., Liu, S., McCutchan, T.F., Pan, W., Xu, W., Li, J., Huang, F., Su, X.. (2015). Regulation of *Plasmodium yoelii* Oocyst Development by Strain- and Stage-Specific Small-Subunit rRNA. *mBio* 6(2). <https://doi.org/10.1128/mbio.00117-15>
17. Spaendonk, R. M. ten, Ramesar, J., Janse, C. J., & Waters, A. P. (2000). The rodent malaria parasite *Plasmodium berghei* does not contain a typical O-type small subunit ribosomal RNA gene. *Molecular and Biochemical Parasitology*, 105(1), 169–174. [https://doi.org/10.1016/s0166-6851\(99\)00180-3](https://doi.org/10.1016/s0166-6851(99)00180-3)
18. Wong, W., Bai, X., Brown, A., Fernandez, I., Hanssen, E., Condrón, M., Tan Y., Baum, J., Scheres, S.. (2014) Cryo-EM structure of the *Plasmodium falciparum* 80S ribosome bound to the anti-protozoan drug emetine. *eLife*. <https://doi.org/10.7554/eLife.03080>
19. Gardner, M. J., Hall, N., Fung, E., White, O., Berriman, M., Hyman, R. W., et al. (2002). Genome sequence of the human malaria parasite *Plasmodium falciparum*. *Nature*, 419(6906), 498–511. <https://doi.org/10.1038/nature01097>
20. Amos, B., Aurrecochea, C., Bah, S., Barba, M., Barreto, A., Basenko, E. Y., Belnap, R., Blevins, A., Böhme, U., Brestelli, J., Brown, S., Callan, D., Campbell, L. I., Christophides, G. K., Crouch, K., Davison, H. R., DeBarry, J. D., Demko, R., Doherty, R., . . . Zheng, J. (2024). VEuPathDB: The eukaryotic pathogen, vector, and host bioinformatics resource center in 2023. *Nucleic Acids Research*, 52(1). <https://doi.org/10.1093/nar/gkad1003>
21. Milligan, J. F., Groebe, D. R., Witherell, G. W., & Uhlenbeck, O. C. (1987). Oligoribonucleotide synthesis using T7 RNA polymerase and synthetic DNA templates. *Nucleic acids research*, 15(21), 8783–8798. <https://doi.org/10.1093/nar/15.21.8783>

22. Clements, R. L., Morano, A. A., Navarro, F. M., McGee, J. P., Du, E. W., Streva, V. A., Lindner, S. E., & Dvorin, J. D. (2022). Identification of basal complex protein that is essential for maturation of transmission-stage malaria parasites. *Proceedings of the National Academy of Sciences*, *119*(34), e2204167119.
<https://doi.org/10.1073/pnas.2204167119>
23. Wostenberg, C., Lary, J. W., Sahu, D., Acevedo, R., Quarles, K. A., Cole, J. L., & Showalter, S. A. (2012). The Role of Human Dicer-dsRBD in Processing Small Regulatory RNAs. *PLOS ONE*, *7*(12). <https://doi.org/10.1371/journal.pone.0051829>
24. Locati, M. D., Pagano, J. F. B., Girard, G., Ensink, W. A., van Olst, M., van Leeuwen, S., Nehrdich, U., Spaink, H. P., Rauwerda, H., Jonker, M. J., Dekker, R. J., & Breit, T. M. (2017). Expression of distinct maternal and somatic 5.8S, 18S, and 28S rRNA types during zebrafish development. *RNA*, *23*(8), 1188–1199.
<https://doi.org/10.1261/rna.061515.117>

ACADEMIC VITA

Leena Wardeh

570 - 492 - 3610 | l.wardeh45@gmail.com

EDUCATION

The Pennsylvania State University Schreyer Honors College **University Park, PA**
Eberly College of Science | B.S. in Biology - Vertebrate Physiology *May 2024*
College of the Liberal Arts | Minor in Anthropology *May 2024*

Danville Area Senior High School **Danville, PA**
High School Diploma *June 2020*

LEADERSHIP EXPERIENCE

Refugee Fundraiser Founder **State College, PA**
SeeNoEvil Jewelry *Apr 2019 - Present*
www.seenoeviljewelry.com

- Created a jewelry fundraiser containing pieces that embrace artistic styles that originate from the Middle East
- Efforts done to raise money and awareness for displaced Syrian refugees, with all proceeds and donations sent to the United Nations High Commissioner for Refugees (UNHCR) & the Aga Khan Foundation

Vice President of Membership Recruitment **University Park, PA**
Alpha Phi Penn State Executive Board *Nov 2021 - Jan 2023*

- Facilitated recruitment exercises for 200 Alpha Phi members on a weekly basis and supervised formal and informal recruiting events for 2,000+ potential new members of the Penn State Panhellenic Community during 2022 and 2023 recruitment

Director of Formal Recruitment **University Park, PA**
Alpha Phi Penn State Recruitment Team *Aug 2021 - Feb 2022*

- Worked alongside the chapter president to carry out 2022 Formal Recruitment and Continuous Open Bidding (COB) through potential member screening, semi-structured interviewing, and member selecting

Class of 2020 Secretary **Danville, PA**
Danville Area Senior High School *Oct 2018 - June 2020*

- Collaborated closely with the class president and vice president to plan and execute class events, fundraisers, and activities, resulting in memorable class experiences for all students

Ski Club President **Danville, PA**
Danville Area Senior High School *Aug 2019 – Feb 2020*

- Fostered a thriving community of skiing enthusiasts through strategic planning, event coordination, and member engagement, resulting in increased membership and successful ski trips and activities

RESEARCH EXPERIENCE

Penn State Huck Center for Malaria Research

University Park, PA

Undergraduate Researcher in the Lindner Laboratory

Aug 2022 - Present

- Pursuing an honors thesis project investigating the translational specialization of *Plasmodium*, the causative agent of malaria
- Actively participating in experimentation using the following procedures: DNA sequencing, RNA extraction, denaturing PAGE, RNA pull-down assays, rodent handling, mass spectrometry, and transmission and analysis of *Plasmodium*

Erickson Discovery Grant Summer Fellowship

University Park, PA

Independent Researcher, and Grant Recipient

Apr 2023 - July 2023

- Awarded \$3,500 to continue an independent research project under the Lindner Laboratory during the summer of 2023
- Focused my research project within the field of parasitology and investigated the specialized function of temporally expressed ribosomes in *Plasmodium yoelii*

Henry Hood Center for Health Research

Danville, PA

Mirshahi Laboratory Research Student

Aug 2019 - Feb 2020

- Volunteered in studies involving mutating and tagging different proteins in hospital patient DNA to see if mutations contributed to coronary disease development
- Developed proficiency in the following skills: pipetting, centrifuge samples, cell fractionation, gel electrophoresis, bacterial culture, DNA extraction, creating stock & preparing plates, diluting solutions, sample washing, autoclave instruments, cell imaging

PROFESSIONAL EXPERIENCE

Penn State Department of Biology

University Park, PA

BIOL 110 Lab Teaching Assistant

Aug 2021 - Dec 2023

- Facilitating an active and conducive learning environment for students to develop fundamental biological laboratory skills
- Grading assignments and lab reports while advising students during office hours on how to develop learning and studying strategies throughout the semester

Penn State Department of Chemistry

University Park, PA

Organic Chemistry I and II Grader

Aug 2022 - Dec 2023

- Providing valuable feedback and assessment to undergraduate organic chemistry students on their coursework and examinations, ensuring the maintenance of academic standards

Geisinger Medical Center Volunteer Services

Shamokin, PA

Adult Hospital Volunteer

June 2019 - Present

- Serving in both clinical and non-clinical placements at two branches of the Geisinger Medical System: The Hospital for Advanced Medicine (Danville, PA) and The Fresh Food Farmacy (Shamokin, PA)

MOHS Dermatology and Internal Medicine Observership

Danville, PA

Geisinger Outpatient Woodbine Clinic

June 2022 - Aug 2022

- Observed both initial MOHS procedure and check-up visits between licensed MOHS dermatologist (Dr. Petrick) and patients
- Observed both minor procedures and check-up visits between licensed internists (Dr. Miller, Dr. Al-Agha, Dr. Wardeh) and patients

Wardeh-Agha Medical Center, LLC

Shamokin, PA

Medical Assistant

Aug 2019 - Feb 2021

- Documented patient charts while working closely with both physicians and nurses to improve overall productivity, efficiency, and patient healthcare experience
- Interacted with and assisted patients ranging from 20 to 90 years old while recording their preliminary vitals

The Tavern at Pine Barn Inn

Danville, PA

Hostess & Waitress

May 2021 - Dec 2021

- Managed the reservation system efficiently, accurately recording bookings and optimizing table turnover rate
- Provided exemplary table service, taking orders, and delivering food and beverages with attention to detail and accuracy

Sunnybrook Park and Pool

Danville, PA

Lifeguard

May 2019 - Aug 2020

- Supervised groups of 20-40 children ages 3-18 while organizing events and activities
- Regulated pool pH at several points throughout each workday using acid/base chemistry

EXTRACURRICULAR ACTIVITIES

Friends of Doctors Without Borders

University Park, PA

Active Member

May 2023 - Present

- Intending to collaborate with like-minded peers to raise awareness about the organization's humanitarian efforts, fundraising events, and initiatives that support Doctors Without Borders' life-saving missions worldwide

Penn State Society of Community Development

University Park, PA

Active Member

Mar 2023 - Present

- Intending to initiate impactful community-driven projects, promote sustainable development, and facilitate collaborative partnerships with local organizations

Penn State THON

University Park, PA

Alpha Phi and Alpha Epsilon Pi

Feb 2021 - Present

- Actively participating in fundraising and awareness to support pediatric cancer as a part of the largest student-run philanthropy in the world
- Providing emotional and financial support on behalf of Alpha Phi to five families with children who had or currently fight against pediatric cancer (the Smiths, McDonnells, Zomoks, DiRoccas, and Fischmans)

Alpha Epsilon Delta Pre-Medical Honors Society
Nationally Inducted Member and Pre-Medicine Mentor

University Park, PA
Sept 2020 – Present

- Currently serving as a mentor for first-year pre-medical students through the Peer Mentoring Program
- Nationally inducted member by meeting the academic standards of the National Health Professional Honor Society

CONFERENCES ATTENDED

Pennsylvania Parasitology Conference
The Huck Institutes of the Life Sciences

University Park, PA
July 21 - 22, 2023

- Presented a research poster titled "Exploring the Specialization of Temporally Expressed *Plasmodium* Ribosomes" showcasing the results of my dedicated summer research efforts
- Gained valuable insights from leading experts in the latest advancements in parasitology and met fellow researchers in the field

Alpha Phi Executive Leadership Conference
Alpha Phi International 2022

East Rutherford, NJ
Feb 25 - 27, 2022

- Represented Penn State Alpha Phi as VP of Membership Recruitment and gained valuable insights, best practices, and innovative strategies that elevated our chapter's recruitment process and enhanced member engagement

Future Business Leaders of America State Conference
FBLA Pennsylvania Chapter

Hershey, PA
April 8 - 10, 2018 | April 7 - 9, 2019

- Represented Danville Area Senior High School, engaged in competitive events, and gained valuable insights into the world of business and entrepreneurship

LANGUAGES

Type: Arabic **Skill Level:** Advanced Understanding/Proficient Speaking

AWARDS

- **2024 Penn State Office of Science Engagement Research Grant**
- **2023 Penn State Schreyer Honors College Research Grant**
- **2023 Edward C. Hammond Jr. Memorial Scholarship in Eberly College of Science**
- **2023 Erickson Discovery Summer Research Grant**
- **2020 - 2024 Penn State Schreyer Honors College Academic Excellence Scholarship**
- **2020 - 2023 Penn State Eberly College of Science Deans List**
- **2022 Virginia L. Corson Eberly College of Science Scholarship**
- **2020 DHS Class of 1939 Scholarship Fund**